This is an open access article published under an ACS AuthorChoice License, which permits copying and redistribution of the article or any adaptations for non-commercial purposes.

analytical chemistry

Article

pubs.acs.org/ac

Measuring Localized Redox Enzyme Electron Transfer in a Live Cell with Conducting Atomic Force Microscopy

Lital Alfonta,*[,†,‡,#] Brian Meckes,[§,#] Liron Amir,[†,‡] Orr Schlesinger,[†,‡] Srinivasan Ramachandran,[§,∥] and Ratnesh Lal*[,§,∥,⊥]

[†]Department of Life Sciences, [‡]Ilse Katz Institute for Nanoscale Science and Technology, Ben-Gurion University of the Negev, P.O. Box 653, Beer-Sheva, 84105, Israel

[§]Department of Bioengineering, [∥]Department of Aerospace and Mechanical Engineering, [⊥]Materials Science Program, University of California San Diego, 9500 Gillman Dr., La Jolla, California 92093, United States

Supporting Information

ABSTRACT: Bacterial systems are being extensively studied and modified for energy, sensors, and industrial chemistry; yet, their molecular scale structure and activity are poorly understood. Designing efficient bioengineered bacteria requires cellular understanding of enzyme expression and activity. An atomic force microscope (AFM) was modified to detect and analyze the activity of redox active enzymes expressed on the surface of *E. coli*. An insulated gold-coated metal microwire with only the tip conducting was used as an AFM cantilever and a working electrode in a three-electrode electrochemical cell. Bacteria were engineered such that alcohol dehydrogenase II (ADHII) was surface displayed. A quinone, an electron transfer mediator, was covalently attached site specifically to the displayed ADHII. The AFM probe was used to lift a single bacterium off the surface for electrochemical analysis in a redox-free buffer. An electrochemical comparison between two quinone containing mutants with different distances from the NAD^+ binding site in alcohol dehydrogenase II was performed. Electron transfer in redox active proteins showed increased efficiency when mediators are present closer to the NAD^+ binding site. This study suggests that an integrated conducting AFM used for single cell electrochemical analysis would allow detailed understanding of enzyme electron transfer processes to electrodes, the processes integral to creating efficiently engineered biosensors and biofuel cells.

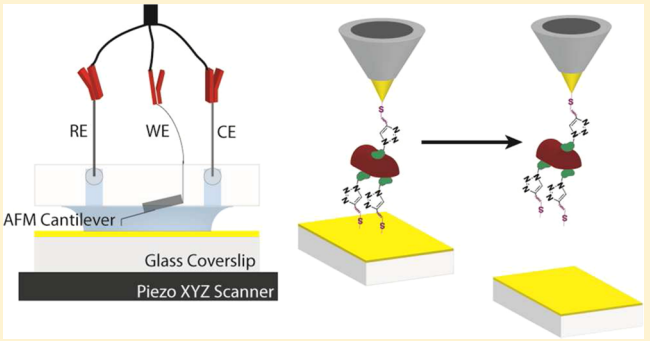

Understanding the electrical and chemical activity of individual cells will play a critical role in designing and developing future bioelectronics. High-resolution functional imaging is critical for understanding molecular scale activity and its underlying structural substrate. Atomic force microscopy (AFM) allows for high resolution imaging as well as simultaneous study of various physicochemical properties.[1−9] Coupling of AFM and electrochemical analysis (EC) has been developed, although mostly for measuring the conductance in nonliving systems.[10−12] It has been used to study diffusional species in solution with the imaged substrate surface acting as a working electrode for self-assembled monolayers on the surface[13] and the switch of redox states of a single metalloprotein bound to the surface.[14] Recently, EC-AFM has been used for potential dependent adsorption/desorption of inorganic molecules.[15] However, selective removal of a single cell from a surface and subsequent electrochemical study of a specific redox protein expressed by the cells has not been reported.

Nicotineamide adenine dinucleotide (NADH) serves as a cofactor in over 300 redox enzymes, including alcohol dehydrogenase II (ADHII), the enzyme of interest in the bacterial system studied here. These dehydrogenases are being used in catalytic electrochemical oxidation processes in biosensors and in biofuel cells among other bioelectronic applications. The large overpotentials that are needed to oxidize NADH to NAD^+ render it useless for these purposes.[16] To overcome overpotentials, it was suggested to modify the surface of an electrode with quinones.[17] In this study and others, the possibility of covalent incorporation of electron-transfer mediating groups attached to the surface of the electrode was suggested and studied. Other studies have demonstrated a remarkable decrease in overpotentials needed for NADH oxidation.[18,19]

We have previously developed a novel approach for bacterial redox enzyme modification and expression.[20] We have shown that these engineered bacteria can be successfully used in a biofuel cell and can even be used as active and viable biocatalysts for more than a week with relatively high power outputs. Briefly, *E. coli* was modified to display the redox

Received: April 29, 2014
Accepted: June 30, 2014
Published: June 30, 2014

 © 2014 American Chemical Society dx.doi.org/10.1021/ac5015645 | *Anal. Chem.* 2014, 86, 7674−7680

enzyme, ADHII, on the surface using an autodisplay system.[21] The unnatural amino acid para-azido-L-phenylalanine (Az) was incorporated into a specific site of the enzyme using the stop codon suppression strategy.[22] When attached to Az a quinone facilitates electron transfer between the enzyme and an electrode. In order to attach the bacteria carrying the surface displayed enzyme to a surface, a quinone linker **1** containing an alkyne and a thiol moiety on opposite ends (**1**) was synthesized and attached to the dehydrogenase site specifically through a copper(I)-catalyzed azide−alkyne cycloaddition reaction.[23] Using this approach, we were able to covalently link bacteria to gold-coated surfaces. The orientation of the redox enzyme on the surface of the electrode can be controlled, and the distances for electron transfer between the enzyme active site and the electrode surface are predetermined.

In order to enable the characterization of the bacterial surface and its electrochemical properties, we have coupled the imaging abilities of atomic force microscopy (AFM) with those of electrochemical techniques. The AFM cantilever, coated in gold and insulated such that the tip is the conducting surface, served both as an imaging probe and as a working electrode in the electrochemical cell. The bacteria express ADHII with a linker **1** attached site specifically to their surface. An exposed thiol on the linker **1** facilitates the gold AFM cantilever attachment to the bacteria. This novel approach was created to determine: (1) What will happen if a quinone is covalently attached site specifically into a predetermined site, in a hydrogenase that uses NAD^+ as its cofactor. (2) How it will affect its oxidation overpotentials. (3) How the distance of the NAD^+ from the electrode surface will affect its electron transfer (ET) properties. Utilizing our modified AFM probes, we successfully imaged and measured the electrochemical activity of a single bacterium with different ADHII mutants. Through these studies, we demonstrated improved activity in ADHII mutants with electron transfer mediators close to the NAD^+ binding site. This approach for studying enzymes can be applied and adapted to study the electrochemistry of other redox enzymes and electrogenic bacteria as well as synthetic electrochemically active nano/microparticles.

EXPERIMENTAL SECTION

Chemicals and Reagents. All chemical reagents were purchased from Sigma-Aldrich (Rehovot, Israel) or Acros (Geel, Belgium) and used without further purification. The unnatural amino acid AzPhe was purchased from Bachem (Bubendorf, Switzerland). PCR was performed with the Kapa HiFi PCR Kit (Kapa Biosystems, Woburn, MA). Plasmid DNA isolation was performed with the QIAprep spin miniprep kit (QIAGEN, Hilden, Germany). Oligonucleotides were supplied by Sigma (Rehovot, Israel) and by IDT (Jerusalem, Israel).

Modified Bacteria Preparations. A full description of modified bacteria can be found in our previous report.[20] Briefly, site-directed mutagenesis on pJM7-ADH (plasmid encoding for Autodisplay of ADHII) was performed using a QuikChange II kit according to the manufacturer's instructions, using the primers for PCR, containing mutation sites for ADHIIV66Az or for ADHIID314Az. (A full list of primers is depicted in ref 20.)

Surface Modifications. Glass microscope slides (Marienfeld, Lauda-Königshofen, Germany) were cleaned using the UVOCS ozone cleaning system (Lansdale, PA) for 10 min. A 5 nm chromium adhesion layer and a 20 nm gold layer were deposited using K575X sputter coater (Quorum Technologies, Kent, UK). Bacteria were attached to the surface as described in ref 20.

Preparation of AFM Probe/Working Electrode. The AFM probe was created utilizing a sharp tungsten wire coated in epoxylite with a shaft diameter of 40 μm (FHC, Bowdoin, ME). Gold was sputtered onto the wire to a thickness of 25−50 nm. The wire was reinsulated through 3 coatings with ClearClad HSR (Chicago, IL) following the manufacturer's instructions. The wire was attached to a custom cantilever holding chip, and a gold mirror was affixed for laser detection with Two-Ton Epoxy (Devcon, Danvers, MA).

AFM Sequence of Operations and Imaging. Images and adhesion measurements were taken with a Multimode AFM with a Nanoscope V controller (Bruker, Santa Barbara, CA). Images were taken with a custom tungsten probe (k = ∼10 N/m) in contact mode with the force minimized to reduce damage to the bacteria. Bacteria were imaged at scan rates of 2−5 Hz. The probe was then zoomed onto a single bacteria, and the scan area was set to 0 μm^2. After localization of bacteria, force images were taken with ramp sizes of 500 nm. The probe remained in contact with the surface with a constant force when initial electrochemical measurements were taken.

Electrochemical Measurements. An EMstat^{3+} potentiostat was used (PalmSens BV, The Netherlands) for cyclic voltammetric measurements. A three-electrode electrochemical cell was assembled where the working electrode was a Tungsten AFM tip coated with gold (Scheme 2). The reference electrode was Ag/AgCl wire prepared by electroplating in 1 M KCl for 30 min at 1 V. The wire was prepared as a reference electrode daily prior to all experiments to reduce electrical drift; a reference solution of 1:1 ratio 10 mM $Fe(CN)_6^{3-/4-}$ in TRIS buffer was made and used daily to verify the reference potential of the reference electrode (Figure S3, Supporting Information). The reference electrode was present with a large junction to allow a large access area. The counter electrode was a platinum wire. All electrodes were assembled in a liquid AFM cell (Bruker, Santa Barbara, CA) equipped with several pores for electrodes. The working volume was ca. 100 μL. Electrolyte solution was 0.1 M Tris buffer, pH = 8.0. Measurements were conducted in the range of −0.8 to 0.1 V vs Ag/AgCl with varying scan rates. Electrode surface area determinations were conducted using a 10 mM solution of $Fe(CN)_6^{3-/4-}$ (1:1 ratio mixed solution), in a range of (−0.1) to (+0.6) V vs Ag/AgCl. Cathodic peaks determination was done by drawing a baseline between forward and reverse curves and measuring the region with the largest current from the baseline for each scan rate. The potential at the largest current point was determined as the cathodic potential, and the current at that point was determined as the cathodic peak current.

RESULTS AND DISCUSSION

Electrochemical Cell Configuration. The electrochemical cell was configured with the gold coated tungsten microwire acting as a cantilever tip while serving as the working electrode in the three-electrode electrochemical cell. The probe was insulated to limit the active electrode area to the tip of the probe (described in the Experimental Section). Platinum and Ag/AgCl wires acted as the counter and reference electrodes, respectively (Scheme 1). The Ag/AgCl wire was placed directly in contact with the fluid creating a large access junction to prevent junction clogging as would occur in a small junction glass electrode.

dx.doi.org/10.1021/ac5015645 | Anal. Chem. 2014, 86, 7674−7680

Scheme 1. Schematic Description of the EC-AFM Setup[a]

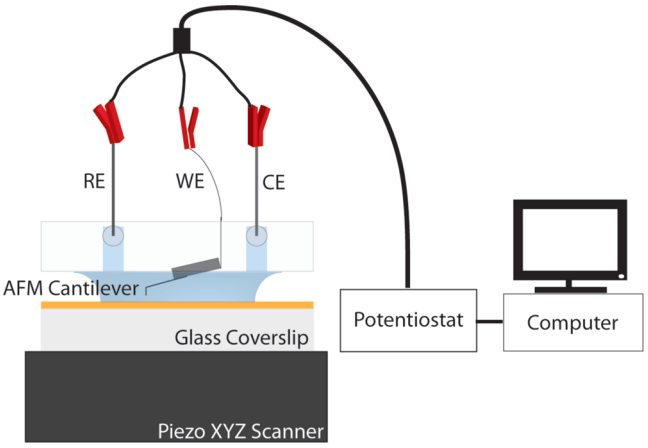

[a]The materials for the electrodes, reference (RE), working (WE), and counter (CE), were Ag/AgCl, Au, and platinum, respectively.

Imaging of Bacteria. Three different mutants of alcohol dehydrogenase II (ADHII) were displayed on the surface of *E. coli*. Each mutant was generated with varying distances from the NAD^+ binding pocket; mutants V66Az and P182Az were generated with approximate distances of ~5 Å each from the binding pocket and mutant D314Az with a distance of ~42 Å from the binding pocket (Figure S1, Supporting Information). In this study, we have excluded mutant P182Az as V66Az is a similar distance (~5 Å) from the NAD^+ binding pocket. The modified bacteria were covalently attached to gold-sputtered glass slides via linker **1**. Slides with attached bacteria were imaged with the wire AFM cantilever. Figure 1A shows an image of multiple bacteria on the surface of a slide. A bacterium was localized with the AFM for subsequent electrochemical analysis. Figure 1B–D shows individual bacterium of different mutants, V66Az, D314Az, and wild type bacteria (WT), selected for electrochemical measurements. The presence of bacteria on the gold substrates was confirmed with light microscopy imaging (Figure 1E).

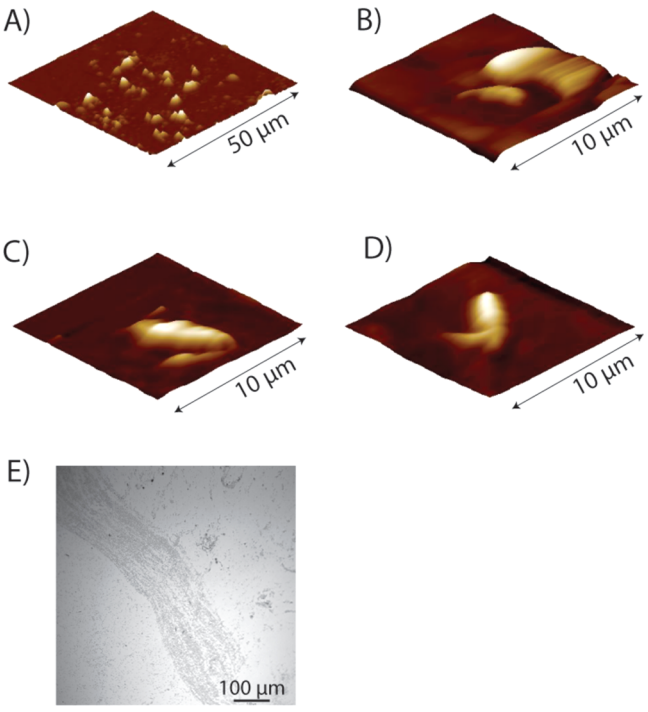

Figure 1. AFM images of the different stages of surface and tip manipulations. (A) Large scan area with D314Az mutant bacteria. (B–D) Scans of single bacterium used in electrochemical measurements of V66Az (B), D314Az (C), and WT (D). (E) Light microscopy images of bacteria attached to the gold substrate.

Picking up a Single Bacterium. A bacterium was picked up by the conducting AFM probe through the following steps as summarized in Scheme 2. After localization of a bacterium, the gold-coated conducting AFM probe was allowed to remain in controlled contact with the bacterium surface without imaging to facilitate gold–thiol bond formation between the linker **1** site specifically attached to ADHII and the probe for ~5 min (Scheme 2B). The chemical structure of the thiol containing linker **1** is shown in the inset of Scheme 2. The tip was then disengaged from the surface (Scheme 2C). Successful attachment of the bacterium to the tip inhibited reimaging of the surface. This was further confirmed through observed changes in cyclic voltammograms. The activity of the probe before imaging the bacteria was recorded (Figure 2, background). During the selection of a single bacterium, electrochemical measurements were conducted to check whether electrochemical activity could be detected (Figure 2, surface mode). This served as our first indication of a successful transfer of a bacterium from the surface to the tip. Upon selecting and attaching a bacterium to the AFM tip, we commenced with our electrochemical analysis of electron transfer (ET) processes (Figure 2, withdrawn mode). Coupling both the AFM imaging abilities with the electrochemical signals demonstrated that we have collected a redox active bacterium off the surface. However, this did not exclude the possibility that only part of the bacteria was removed.

In order to ascertain gold–thiol bond formation between the enzymes on the bacterial surface and the cantilevered tip, we measured the adhesion forces while engaging a single bacterium. Figure 3 shows examples of the measured adhesion using the force mode for mutants D314Az and V66Az. As a control measurement, adhesion forces were also measured for a bare Au surface. In addition, only upon observing these adhesion forces could electrochemical activity be detected on the surface of the AFM tip (serving as our working electrode). Combining all this evidence together with the actual size of our working electrode (ca. 100 μm^2) indicates that the probe and system is capable of picking up a single bacterium or a fragment. Control experiments conducted with surfaces modified with WT nonmodified bacteria that were nonspecifically bound to the surface as well as surface modified bacteria displaying WT-ADHII did not yield any visible electrochemical signals. This occurred neither when the probe engaged the bacteria on the surface nor when the probe was subsequently withdrawn.

Determination of Electrode Size and Surface Coverage. Due to the fabrication processes and customization of the working electrodes for AFM, there existed heterogeneity in electrode surface areas. In order to avoid large differences between the measured surfaces, we have used a 10 mM solution of $Fe(CN)_6^{3-/4-}$ for an initial determination of our actual active surface, basing our calculations on the Randles-Sevcik equation for diffusional species. Thus, tips that have shown large redox currents indicating surface areas larger than 100 μm^2 were excluded.

dx.doi.org/10.1021/ac5015645 | *Anal. Chem.* 2014, 86, 7674–7680

Scheme 2. Description of the Sequence of Operations Conducted in Order to Lift a Single Bacterium off the Surface Using an AFM Gold Coated Tip

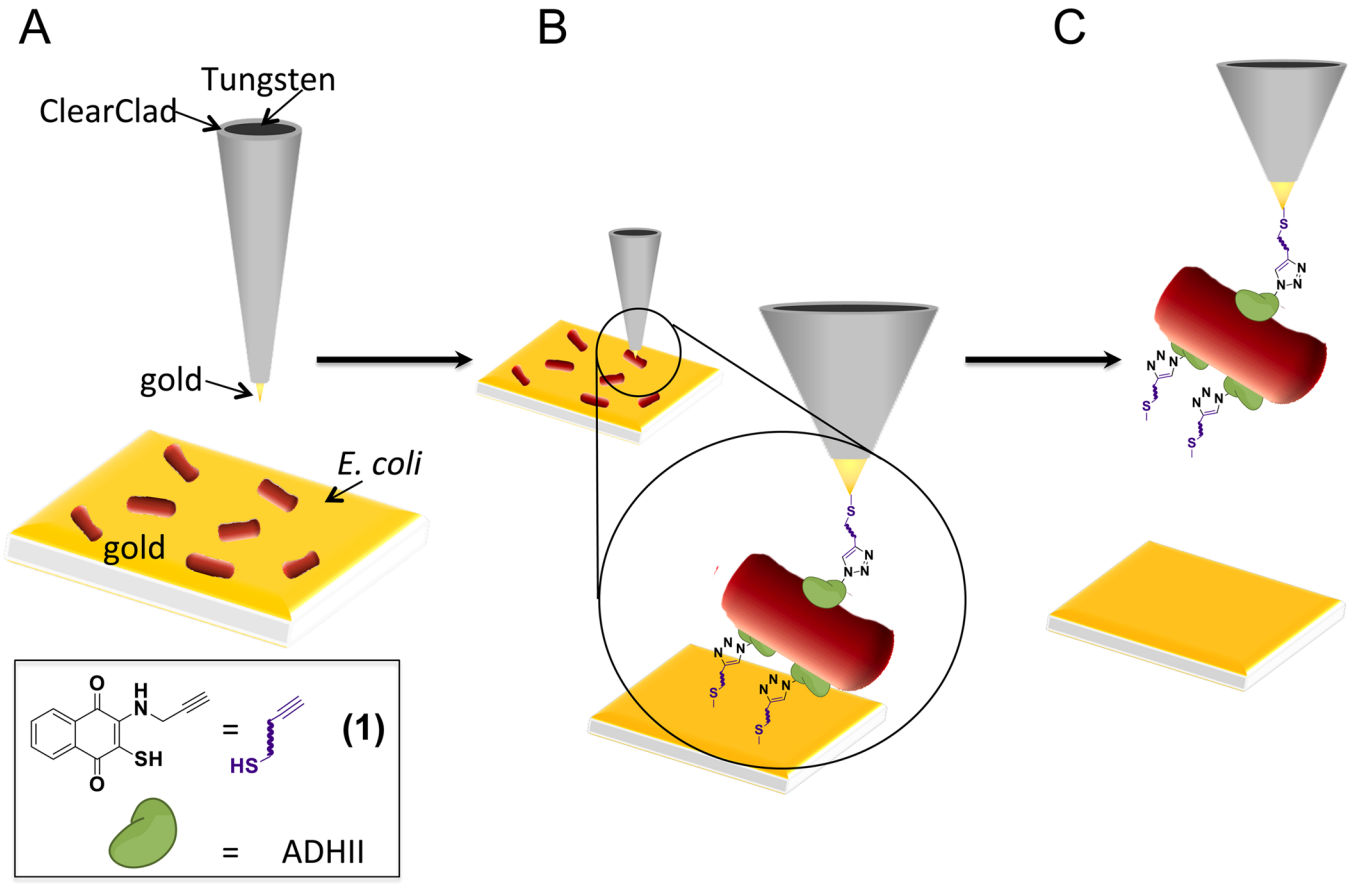

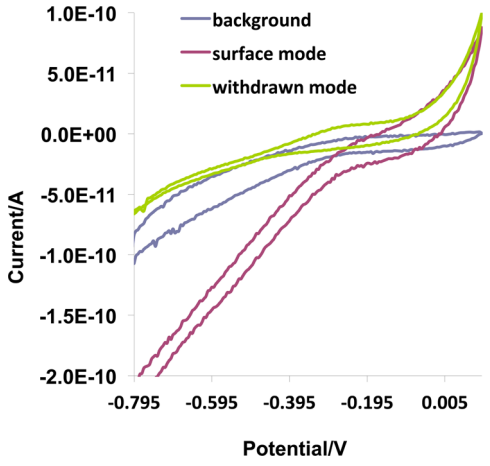

Figure 2. Cyclic voltammograms collected at every mode of bacterium selection. Background: before engaging the surface. Surface mode: engaging with a single bacterium. Withdrawn mode: withdrawing upon attachment of a bacterium. Scan rates were 0.05 V s^{-1}; reference electrode: Ag/AgCl wire.

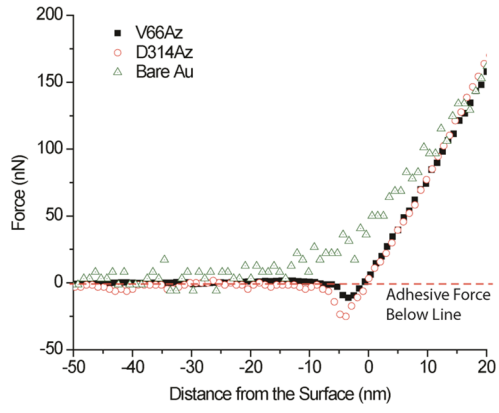

Figure 3. AFM retraction curves are shown for ADHII mutants V66Az and D314Az during cantilever attachment to a single bacterium. Adhesion forces are visible for both mutants. Bare gold substrates are shown as a control.

Figure 4 shows the cyclic voltammograms collected using a mutant V66Az modified AFM tip (lavender colored line), a mutant D314Az modified tip (rose colored line), and a background measurement of the unmodified working electrode (lime green colored line) collected at a scan rate of 0.05 V s^{-1}. When studying the electrochemical properties of linker **1**, based on eq 1, plotted I_p values against scan rates determined a surface coverage of $\Gamma = 2.3 \times 10^{-10}$ mol·cm^{-2}. However, surface coverage values calculated for the surface modified bacteria containing linker **1** bound to the surface of the electrode yielded values of $\Gamma_o = 8.0 \times 10^{-11}$ mol·cm^{-2} and $\Gamma_R = 1.0 \times 10^{-11}$ mol·cm^{-2} for mutant V66Az, oxidized and reduced forms, respectively, whereas the values of surface coverage for mutant D314Az were $\Gamma_o = 2.7 \times 10^{-11}$ mol·cm^{-2} and $\Gamma_R = 8.0 \times 10^{-12}$ mol·cm^{-2}, for the oxidized and reduced forms. The much lower conversion values for the mutants, compared to those measured for linker **1** by itself, suggest that there is an additional process

dx.doi.org/10.1021/ac5015645 | *Anal. Chem.* 2014, 86, 7674−7680

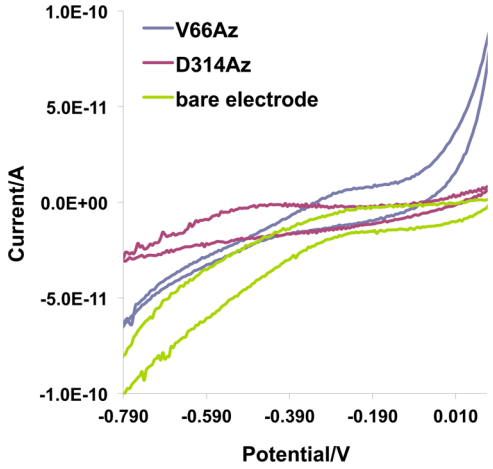

Figure 4. Cyclic voltammograms of the different mutants; lavender colored line: mutant V66Az; rose colored line: mutant D314Az; lime green colored line: background measurement with an unmodified working electrode. Scan rates were 0.05 V s^{-1}; reference electrode: Ag/AgCl wire.

that is involved, namely, the redox reaction of NADH. Taking into account the redox potential measured for mutant D314Az and the fact that it is identical to the redox potential of linker **1**, but with much lower reversibility, it is suggested that the degree of mediation of ET between NAD^+ and the quinone containing linker is much lower than for mutant V66Az.

Using the calculated values based on eq 1 and knowing the approximate surface area of our electrode, we could estimate the number of active enzymes bound to the surface.

$$I_p = \frac{[n^2F^2\Gamma A\upsilon]}{4RT} \quad (1)$$

where I_p is the current at the peak (anodic peak or cathodic peak), n is the number of electrons in the reaction, F is the Faraday constant, R is the gas constant, T is the temperature in Kelvin (in this case, 298 K), A is the electrode surface area in cm^2, Γ is the surface coverage in mol·cm^{-2} for the anodic or the cathodic process, and υ is the potential scan rate in V s^{-1}.

These values can be translated to the number of redox active enzyme copies displayed per bacterium that varied between ~160 000 copies for bacteria displaying mutant D314Az and ~480 000 copies for bacteria displaying mutant V66Az. These numbers are in good agreement with the reported performance of the bacterial autodisplay system.[24] However, these numbers do not agree with our previously reported numbers based on our attachment of gold nanoparticles to the enzymes and a cautious count of the number of nanoparticles, when we reported an approximate 11 000 copies per cell.[20] The difference could stem from several reasons: one was our avoidance of counting gold nanoparticles that have aggregated, and another could be that gold nanoparticles failed to bind all displayed enzymes.

ET Measurements and Mutants Comparison. We have used Laviron's analytical approach for cases of peak to peak separation of ΔE_p > 200 mV/n (n being the number of electrons)[25] to calculate the transfer coefficient α and the apparent rate constant k_{app} for mutants V66Az and D314Az. We did not conduct calculations for mutant P182Az since it has exhibited similar peak potentials as mutant V66Az, probably due to similar distances from the NAD^+ binding pocket. Figure 5A shows the voltammograms collected upon picking up a

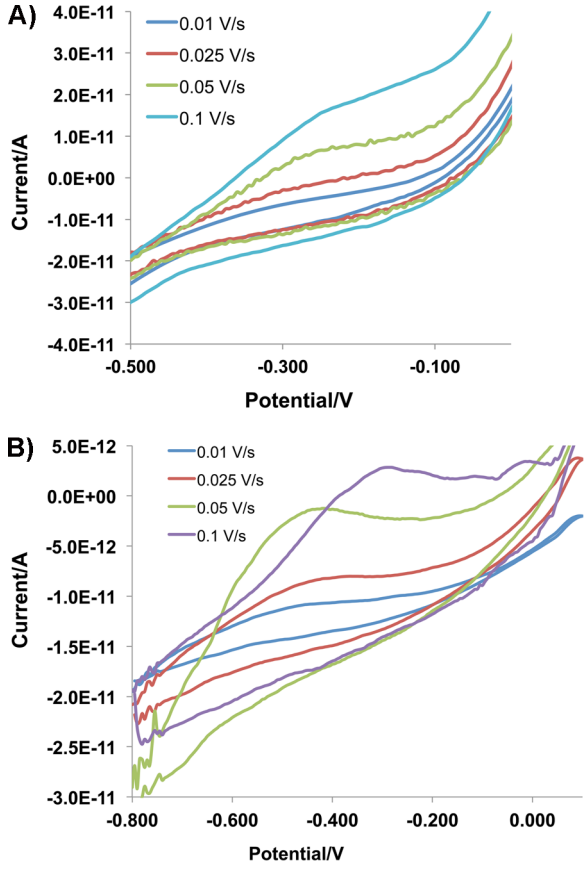

Figure 5. (A) Cyclic voltammograms conducted under different scan rates for mutant V66Az. (B) Cyclic voltammograms conducted under different scan rates for mutant D314Az. The range was limited to emphasize the peaks. The full scale is shown in Figure S2A,B, Supporting Information.

bacterium that displayed ADHII mutant V66Az on its surface. Due to very low peak currents compared to catalytic currents present in the voltammograms, we are not showing the full range of potentials that were scanned in each experiment, only the region in which the peaks have appeared (the full scale voltammograms are shown in Figure S2A, Supporting Information). For mutant V66Az, the formal potential, $E^{0\prime}$ was calculated to be −250 mV vs Ag/AgCl. This relatively high potential is an indication that indeed the electrons are being transferred from NADH through the quinone and not just from the quinone that is directly bound to the surface. The middle point potential that was measured for the quinone used in this study is −350 mV vs Ag/AgCl (Figure S2B, Supporting Information). Transfer coefficients α and $1 - \alpha$ were calculated to be 0.4 and 0.6, respectively, whereas k_{app}, the electron transfer rate constant, varied in the different measurements between 5.6 and 7.2 s^{-1}. These values are in good agreement with values reported in the literature for electrodes modified with quinone derivatives to mediate NADH enzymatic oxidation, where the enzymes were randomly oriented relative to the electrode.[26] These values are significantly higher than values reported for ADH/toluidine blue O/nafion electrodes modified nonspecifically, at a value of 0.12 s^{-1}.[19]

The same measurements were conducted with surfaces modified with bacteria displaying mutant D314Az (Figure 5B). The measured formal potential was $E^{0\prime}$ = −350 mV vs Ag/AgCl. Since this potential is the same as the one that we have

dx.doi.org/10.1021/ac5015645 | Anal. Chem. 2014, 86, 7674−7680

measured for linker **1** alone, we assume that we have measured in this case the ET process between the quinone and the electrode almost exclusively without the ability to successfully mediate ET between the quinone and the NAD^+ in the remote binding pocket. Using Laviron's approach for the analysis of the ET process for this mutant, the transfer coefficients, α and $1 - \alpha$, were calculated to be 0.15 and 0.85, respectively. The measured k_{app} was 1.2−1.5 s^{-1}. Here, we must note that the measurements for the cathodic peaks of both mutants were done by a mathematical deconvolution (detailed explanation appears in the Experimental Section) due to reductive catalytic peaks that appeared in more negative potentials probably due to bacterial lysis on the surface. Furthermore, due to a very small number of redox active molecules on the surface (in the range of hundreds of thousands only per measurement), measured currents are extremely low, in the picoampere range, the limit of our measuring abilities. Nonetheless, in the region of middle point potentials, a marked increase in capacitive currents was observed, which lead us to believe that a Faradaic process is taking place in that region. Lysis of bacteria may occur due to large forces applied to bacteria by the AFM tip during imaging caused by the relatively high stiffness of the probe.

The k_{app} value calculated for linker **1** when it was bound to the electrode surface varied between 5.75 and 7.5 s^{-1} in our different measurements with a surface coverage that is about 2.3×10^{-10} mol·cm^{-2}, whereas surface coverage of mutant D314Az was an order of magnitude lower, with a much lower ET rate constant (within the error of the measurement). This value is lower than that calculated for mutant V66Az, where the mediated ET is evident due to the very low conversion rate between oxidized and reduced forms as well as the positively shifted middle point potential. All of these results together strengthen our conclusion that the NADH is hardly involved in this reaction (using mutant D314Az) since it is too far (at least 42 Å away from the quinone). Our earlier studies with the same mutants have shown much lower bioelectrocatalytic activity for mutant D314Az.[20]

CONCLUSIONS

Using an integrated conducting AFM for single cell electrochemical analysis, we were able to obtain a detailed understanding of enzyme electron transfer processes to electrodes. We were able to determine the surface coverage of the electrode and, by imaging a single bacterium, calculate the number of surface displayed redox enzymes for the first time without using biochemical tools. We could study different mutants and their characteristic ET rate constants as well as redox potentials. Through multidimensional experimental results, we were able to show that, when the distance between a mediator and an active enzyme binding pocket is too large, hardly any mediation occurs. In contrast, when the distance between the enzymatic active site and the redox mediator is small (5 Å in this case), mediation of ET occurs that is reflected in the fast ET as predicted by theory. The surface density by the autodisplayed enzymes is very close to surface densities reported for enzymatic electrodes that contained ADH with larger dimensions.[19] These results strongly suggest that the enzyme expression density in our system is relevant for studies using "enzymatic-like" electrodes. In summary, our combined AFM-electrochemical system can be used as a platform for single cell analysis of enzyme activity; such information is critical for efficient design, development, and study of bioelectronic systems.

ASSOCIATED CONTENT

Supporting Information

Additional information as noted in text. This material is available free of charge via the Internet at http://pubs.acs.org.

AUTHOR INFORMATION

Corresponding Authors

*E-mail: alfontal@bgu.ac.il.

*E-mail: rlal@ucsd.edu.

Author Contributions

#L. Alfonta and B. Meckes contributed equally.

Notes

The authors declare no competing financial interest.

ACKNOWLEDGMENTS

Research leading to these results received funding from the European Research Council ERC grant agreement no. 260647 (L. Alfonta) as well as the Safra Center for the study and engineering of functional biopolymers at BGU (L. Alfonta). L. Alfonta is the incumbent of the Elaine S. and Alvin W. Wene Career Development Chair in Biotechnology Engineering. L. Amir acknowledges a Converging Technologies and a Kreitman school for graduate students Negev fellowships. A Merage Ph.D. fellowship from the Ilse Katz Institute for Nanoscale Science and Technology is acknowledged (O.S.). Research reported in this publication was supported by the National Institute on Drug Abuse of the National Institutes of Health under award numbers R01DA025296 (R.L.), R01DA024871 (R.L.), and F31DA034562 (B.M.). We gratefully acknowledge Prof. Peter G. Schultz for providing the pSup-MjAzRS-6TRN plasmid, Prof. Thomas Meyer for generously providing *E. coli* JK321 strain and pJM7 plasmid, and Prof. Yuval Shoham for the *Z. mobilis* genome. We also thank Mr. Nirav Patel for technical assistance.

REFERENCES

(1) Binnig, G.; Quate, C. F.; Gerber, C. *Phys. Rev. Lett.* **1986**, *56*, 930−933.

(2) Hansma, P. K.; Drake, B.; Marti, O.; Gould, S. A.; Prater, C. B. *Science* **1989**, *243*, 641−643.

(3) Bard, A. J.; Fan, F. R.; Pierce, D. T.; Unwin, P. R.; Wipf, D. O.; Zhou, F. *Science* **1991**, *254*, 68−74.

(4) Lal, R.; John, S. A. *Am. J. Physiol. Cell Physiol.* **1994**, *266*, C1−C21.

(5) Proksch, R.; Lal, R.; Hansma, P. K.; Morse, D.; Stucky, G. *Biophys. J.* **1996**, *71*, 2155−2157.

(6) Cross, S. E.; Jin, Y.-S.; Rao, J.; Gimzewski, J. K. *Nat. Nanotechnol.* **2007**, *2*, 780−783.

(7) Fantner, G. E.; Barbero, R. J.; Gray, D. S.; Belcher, A. M. *Nat. Nanotechnol.* **2010**, *5*, 280−285.

(8) Connelly, L.; Meckes, B.; Larkin, J.; Gillman, A. L.; Wanunu, M.; Lal, R. *ACS Appl. Mater. Interfaces* **2014**, *6*, 5290−5296.

(9) Meckes, B.; Arce, F. T.; Connelly, L. S.; Lal, R. *Sci. Rep.* **2014**, *4*, 4454.

(10) Bearinger, J. P.; Orme, C. A.; Gilbert, J. L. *Surf. Sci.* **2001**, *491*, 370−387.

(11) Szunerits, S.; Pust, S. E.; Wittstock, G. *Anal. Bioanal. Chem.* **2007**, *389*, 1103−1120.

(12) Davoodi, A.; Pan, J.; Leygraf, C.; Norgren, S. *Electrochem. Solid-State Lett.* **2005**, *8*, B21−B24.

(13) Wold, D. J.; Frisbie, C. D. *J. Am. Chem. Soc.* **2001**, *123*, 5549−5556.
(14) Davis, J. J.; Morgan, D. A.; Wrathmell, C. L.; Axford, D. N.; Zhao, J.; Wang, N. *J. Mater. Chem.* **2005**, *15*, 2160−2174.
(15) Masuda, T.; Ikeda, K.; Uosaki, K. *Langmuir* **2013**, *29*, 2420−2426.
(16) Elving, P. J.; Schmakel, C. O.; Santhanam, K. S. V.; Zuman, P. *CRC Crit. Rev. Anal. Chem.* **1976**, *6*, 1−67.
(17) Tse, D. C.-S.; Kuwana, T. *Anal. Chem.* **1978**, *50*, 1315−1318.
(18) Jaegfeldt, H.; Kuwana, T.; Johansson, G. *J. Am. Chem. Soc.* **1983**, *105*, 1805−1814.
(19) Periasamy, A. P.; Umasankar, Y.; Chen, S.-M. *Talanta* **2011**, *83*, 930−936.
(20) Amir, L.; Carnally, S. A.; Rayo, J.; Rosenne, S.; Yerushalmi, S. M.; Schlesinger, O.; Meijler, M. M.; Alfonta, L. *J. Am. Chem. Soc.* **2013**, *135*, 70−73.
(21) Maurer, J.; Jose, J.; Meyer, T. F. *J. Bacteriol.* **1997**, *179*, 794−804.
(22) Chin, J. W.; Santoro, S. W.; Martin, A. B.; King, D. S.; Wang, L.; Schultz, P. G. *J. Am. Chem. Soc.* **2002**, *124*, 9026−9027.
(23) Kolb, H. C.; Finn, M. G.; Sharpless, K. B. *Angew. Chem., Int. Ed.* **2001**, *40*, 2004−2021.
(24) Jose, J.; Maas, R. M.; Teese, M. G. *J. Biotechnol.* **2012**, *161*, 92−103.
(25) Laviron, E. *J. Electroanal. Chem.* **1979**, *101*, 19−28.
(26) Gorton, L. *J. Chem. Soc., Faraday Trans. 1* **1986**, *82*, 1245−1258.